32nd URSI GASS, Montreal, 19–26 August 2017

Computationally Efficient Near-field Radio Frequency Source Localisation

Jan-Willem W. Steeb*(1), David B. Davidson(1), and Stefan J. Wijnholds(2)(1)
(1) Department of Electrical & Electronic Engineering, Stellenbosch University, South Africa
(2) Netherlands Institute for Radio Astronomy (ASTRON), The Netherlands

Abstract

Radio frequency interference (RFI) is an ever-increasing problem for remote sensing and radio astronomy, with radio telescope arrays especially vulnerable to RFI. Localising the RFI source is the first step to dealing with the culprit system. In this paper, a new near-field localisation algorithm for interferometric arrays with low array beam side lobes, is presented. The computational complexity of the algorithm is linear with search grid size compared to the 3D MUSIC method which scales with the cube of search grid size. The trade-off is that the algorithm requires a once-off a priori calculation and storing of weighting matrices. The proposed algorithm has the same accuracy as 3D MUSIC.

1 Introduction

Radio frequency interference (RFI) is an important issue in many areas of scientific research, for example in remote sensing and radio astronomy. The ideal solution is to identify the location of the RFI and then remove it. For arrays with a high sensitivity or a large spatial extend, near-field sources are of particular interest. This is particularly true for large radio astronomical arrays such as the Low Frequency Array (LOFAR) [1] and the Square Kilometre Array (SKA) [2], which span entire continents and therefore detect many RFI signals from TV and radio broadcast towers and even satellites in their near-field. This makes these arrays an excellent proving ground for near-field RFI localisation and mitigation methods.

Current near-field source localisation algorithms either make use of brute force methods (such as MUSIC [7, p. 80-82] where the entire solution space is searched) or exploit the array layout (a common layout is a uniform linear array). Methods that exploit a uniform linear array layout include path following [3] and polynomial rooting [4].

For radio astronomy arrays, brute force methods are computationally expensive due to the large near-field area caused by long baselines. Furthermore, to obtain as much information as possible for imaging (optimising the UV coverage) the array layouts are non-uniform and non-linear. However, radio astronomy interferometric arrays have the advantage that the array beam has low side lobe levels. Therefore, a novel computationally efficient near-field source localisation algorithm is presented which is designed for irregular interferometric arrays and takes advantage of low array beam side lobes.

In this paper, the following notation is used:

$\mathbf{A}$	Bold upper-case letters are matrices. The jk^{th} element is indicated by $\mathbf{A}_{jk}$.
$\mathbf{a}$	Bold lower-case letters are column vectors. The j^{th} element is indicated by $\mathbf{a}_j$.
$\mathbf{I}$	Identity matrix.
$\|\|\cdot\|\|$	Norm of a vector.
$\text{Tr}(\cdot)$	Trace of a matrix.
$\text{diag}(\cdot)$	Converts a vector into a diagonal matrix.
$\angle$	Phase of a complex number.
i	Square root of -1.
c	Speed of light.
$\{\cdot\}^H$	Hermitian transpose of a matrix.
$\{\cdot\}^T$	Transpose of a matrix.
$\{\cdot\}^*$	Complex conjugate of a scalar.
$\Re(\cdot)$	Real part of a complex number.
$\Im(\cdot)$	Imaginary part of a complex number.

2 Data Model

The scenario that is considered is where an array is observing astronomical sources and the measurements are contaminated by a single near-field RFI source. This will later be generalised to multiple RFI sources. The assumption is made that the power of the RFI source is considerably higher than the power from the astronomical sources, therefore the astronomical sources are omitted from the model. Direction dependent effects such as path loss, polarisation mismatch factor, the gain of the antennas and atmospheric effects are not considered. Furthermore, direction independent effects such as the receiver electronics, in particular the low noise amplifiers, are also not considered.

To keep the model simple the output of the array will only be considered for a single frequency channel and polarisation. If the array consists of N_e elements, then at time t the voltage output can be expressed as [5]

$$\mathbf{y}(t) = \mathbf{x}_s(t) + \mathbf{x}_n(t), \tag{1}$$

where $\mathbf{y}(t) = [y_1(t), \ldots, y_{N_e}(t)]^T$ is the vector of the measured array output signals, $\mathbf{x}_s(t) = [s(t-\tau_1), \ldots, s(t-\tau_{N_e})]^T$ is the vector of the delayed RFI signal and $\mathbf{x}_n(t) =$

$[n_1(t),\ldots,n_{N_e}(t)]^T$ is the vector of instrumental noise for each antenna.

For the j^{th} antenna, τ_j is the delay between the source location and the array element and is given by $\tau_j = ||\mathbf{v}_s - \mathbf{v}_j||/c$ where $\mathbf{v}_s$ and $\mathbf{v}_j$ are the position vectors of the RFI source and antenna, respectively. The delayed signal can be approximated by $s(t-\tau_j) \approx s(t)e^{-i2\pi\nu\tau_j}$, where ν is the centre frequency of the channel. This condition is satisfied if $2\pi\Delta\nu\tau_{max} \ll 1$ [6], where $\Delta\nu$ is the signal's bandwidth and τ_{max} is the delay given by the longest baseline (greatest distance between any two antennas). The phase delays of the source can be stacked into a vector that is called the geometric delay vector $\mathbf{a}(\mathbf{v}_s) = [e^{i2\pi\nu\tau_1},\ldots,e^{i2\pi\nu\tau_{N_e}}]^T$. Therefore, the model in equation (1) can be written as

$$\mathbf{y}(t) = \mathbf{a}(\mathbf{v}_s)s(t) + \mathbf{x}_n(t). \tag{2}$$

To create images, interferometric radio astronomy arrays need the covariance matrix of the signals $\mathbf{R} = \mathbb{E}\{\mathbf{y}(t)\mathbf{y}^H(t)\}$, where $\mathbb{E}$ is the expectation. Independence is assumed between the RFI source and the noise, therefore, the covariance matrix of equation (2) is $\mathbf{R} = \mathbf{R}_s + \mathbf{R}_n = \mathbf{a}(\mathbf{v}_s)\sigma_s^2\mathbf{a}^H(\mathbf{v}_s) + \mathbf{R}_n$ where $\sigma_s^2 = \mathbb{E}\{s(t)s^*(t)\}$ is the power of the RFI signal. If N_s RFI signals are present, then the covariance matrix is the sum of the covariance matrices ($\mathbf{R}_{s,j}$) for each signal

$$\begin{aligned}\mathbf{R} &= \sum_{j=1}^{N_s}\mathbf{R}_{s,j} + \mathbf{R}_n = \mathbf{R}_\Sigma + \mathbf{R}_n \\ &= \mathbf{A}(\mathbf{V}_s)\mathbf{S}\mathbf{A}^H(\mathbf{V}_s) + \mathbf{R}_n,\end{aligned} \tag{3}$$

because all the operators used are linear, where $\mathbf{A}(\mathbf{V}_s) = [\mathbf{a}(\mathbf{v}_{s,1}),\ldots,\mathbf{a}(\mathbf{v}_{s,N_s})]$, $\mathbf{V}_s = [\mathbf{v}_{s,1},\ldots,\mathbf{v}_{s,N_e}]$ and $\mathbf{S} = \text{diag}([\sigma_{s,1}^2,\ldots,\sigma_{s,N_e}^2])$. A classical delay beamformer can be used to create a dirty image from the covariance matrix by calculating for every voxel [7, p. 88]

$$J(\mathbf{v}) = \frac{\mathbf{a}^H(\mathbf{v})\mathbf{R}\mathbf{a}(\mathbf{v})}{(N_e)^2}. \tag{4}$$

A peak in this image indicates the position of a source.

3 Proposed Source Localisation Algorithm

The proposed algorithm consists of three stages. The first is preprocessing, which attempts to remove instrumental noise signals and isolate individual RFI sources. This is followed by the intergrating-out-variables method which exploits the low side lobes and produces a good estimate. This is then used as the initial guess for a fast converging iterative method in the final step.

3.1 Stage 1: Preprocessing

The objective of the preprocessing step is to reduce the effect of the instrumental noise signals and isolate individual RFI sources. As the instrumental noise signals of the antennas are not identically distributed, the noise powers in $\mathbf{R}_n$ will differ. However, the assumption is made that the instrumental noise signals of the antennas are independent, therefore $\mathbf{R}_n$ is a diagonal matrix.

To remove the effect of $\mathbf{R}_n$ on $\mathbf{R}$ a statistical method such as factor analysis [8, p.211-232] can be used, which decomposes the $N_e \times N_e$ covariance matrix into $\mathbf{R} = \mathbf{Z}\mathbf{Z}^H + \mathbf{D}$, where $\mathbf{Z}$ is an $N_e \times Q$ matrix and $\mathbf{D}$ is a diagonal $N_e \times N_e$ matrix. If the method is applied successfully $\mathbf{D} \approx \mathbf{R}_n$ and therefore $\mathbf{Z}\mathbf{Z}^H \approx \mathbf{R}_\Sigma$ (see equation (3)). If the columns of $\mathbf{A}(\mathbf{V}_s)$ are linearly independent and $N_s < N_e$, then $Q = N_s$. For the method to converge an upper limit on the number of factors Q, namely $Q < (N_e - \sqrt{N_e})$, is imposed [5].

The columns of $\mathbf{Z}$ are now used to construct new covariance matrices $\mathbf{R}_{f,j} = \mathbf{Z}(:,j)\mathbf{Z}^H(:,j)$. Consequently, the sources are divided between these covariance matrices and in the ideal case, where the columns of $\mathbf{A}(\mathbf{V}_s)$ are orthogonal, each $\mathbf{R}_{f,j}$ will match with an $\mathbf{R}_{s,j}$. In most radio astronomy data sets a single snapshot covariance matrix is affected by one or two RFI sources and even though the columns of $\mathbf{A}(\mathbf{V}_s)$ may not be orthogonal the separation is sufficient that each $\mathbf{R}_{f,j}$ will contain the majority of one source's power. LOFAR data indicates that unwanted direction and direction independent effects have the greatest effect on the amplitude of the elements of $\mathbf{R}_{f,j}$. This effect can be removed by considering only the phase information, $e^{i\angle\mathbf{R}_{f,j}}$.

3.2 Stage 2: Integrating-out-variables

Let the matrix $\mathbf{W} = e^{i\angle\mathbf{R}_{f,j}}$, where $e^{i\angle\mathbf{R}_{f,j}}$ is a result from the preprocessing step. Since $\mathbf{W}$ is Hermitian with no amplitude information, all the information is contained in the top (or bottom) triangular part of $\mathbf{W}$. There is a total of $N_b = (N_e^2 - N_e)/2$ elements in both the triangular parts which is equal to the number of antenna combinations (also called baselines). By stacking the transposed rows of the top triangular part of $\mathbf{W}$, an $N_b \times 1$ vector $\boldsymbol{\beta}$ is created. The classical delay beamformer spectrum can then be rewritten as a sum (omitting the dependency on $\mathbf{v}$)

$$J = \text{Tr}(\mathbf{R}) + 2\sum_{p=1}^{N_b}\left[\Re(\boldsymbol{\beta}_p)\cos(\boldsymbol{\zeta}_p) + \Im(\boldsymbol{\beta}_p)\sin(\boldsymbol{\zeta}_p)\right], \tag{5}$$

where vector $\boldsymbol{\zeta}$ contains the stacked (similar to $\boldsymbol{\beta}$) angle differences $\gamma_j - \gamma_k$ and $\gamma_j = \frac{2\pi\nu}{c}||\mathbf{v} - \mathbf{v}_j||$, where $\mathbf{v}_j$ is the position of the j^{th} antenna. The traditional method to find the location of the source requires that a beamformer must be constructed for every voxel in the near-field (where the number of voxels is dependent on the resolution as well as the size of the near-field). This problem therefore has computational complexity $\mathcal{O}(N_r \times N_\theta \times N_\phi)$.

To reduce the computational complexity of finding a source location from cubic to linear, the proposed method integrates out variables and then only varies one variable to find

the peak. The trigonometric functions in equation (5) can not be analytically integrated, therefore the integration is done numerically once a priori and is stored (the trade off is therefore that the storage requirement increases). The algorithm notation is: N_ϕ is the number of ϕ values in vector $\boldsymbol{\phi}$, N_θ is the number of θ values in vector $\boldsymbol{\theta}$, N_r is the number of r values in vector $\mathbf{r}$ and r_{nf} is the radius of the near-field. Two weighting matrices are calculated a priori:

- $\mathbf{W}_1$ with dimension $2 \times N_b \times N_\phi$: for $\cos(\boldsymbol{\zeta})$ and $\sin(\boldsymbol{\zeta})$, vary $\phi \in [-\pi, \pi]$ and integrate out $\theta \in [0, \pi/2]$[1] and $r \in [0, r_{nf}]$.
- $\mathbf{W}_2$ with dimension $2 \times N_b \times N_\phi \times N_\theta$: for $\cos(\boldsymbol{\zeta})$ and $\sin(\boldsymbol{\zeta})$, vary $\phi \in [-\pi, \pi]$ and vary $\theta \in [0, \pi/2]$[1] and integrate out $r \in [0, r_{nf}]$.

The weighting matrices $\mathbf{W}_1$ and $\mathbf{W}_2$ are calculated only once for a given array and frequency. The steps of the algorithm are:

- Calculate

$$f_1(\boldsymbol{\phi}(k)) = \sum_{p=1}^{N_b} \left[\Re(\boldsymbol{\beta}_p)\mathbf{W}_1(1,p,k) + \Im(\boldsymbol{\beta}_p)\mathbf{W}_1(2,p,k)\right], \tag{6}$$

  for $k = 1, \ldots, N_\phi$. Find the peak of f_1 and the corresponding index i_ϕ of $\boldsymbol{\phi}$.
- Use index i_ϕ to fix ϕ and find the peak of

$$f_2(\boldsymbol{\theta}(k)) = \sum_{p=1}^{N_b} \Big[\Re(\boldsymbol{\beta}_p)\mathbf{W}_2(1,p,i_\phi,k) + \Im(\boldsymbol{\beta}_p)\mathbf{W}_2(2,p,i_\phi,k)\Big], \tag{7}$$

  for $k = 1, \ldots, N_\theta$. Find the peak of f_2 and the corresponding index i_θ of $\boldsymbol{\theta}$.
- Use i_ϕ and i_θ to fix ϕ and θ, respectively, and use one dimensional classical delay beamforming imaging to obtain a value for r. If the recovered value is not close to 1, return to the first step and choose the next highest peak (and repeat this N_i times until the threshold is met or there are no more peaks).

The position obtained is just an estimate and the accuracy is dependent on how low the side lobe levels are. This method only needs to search an $(N_r + N_\theta + N_\phi)$ array N_i times, while 3D MUSIC must search a 3 dimensional grid $(N_r \times N_\theta \times N_\phi)$. In the simulation results it is shown that N_i is almost always equal to 1.

3.3 Stage 3: Minimum Error Convergence

The proposed convergence algorithm uses the same concepts as those found in [9] which are used for antenna position calibration. The core idea is that $\mathbf{a}(\mathbf{v})\mathbf{a}^H(\mathbf{v})$ can be linearised if the error of the estimate of $\mathbf{v}_s$ is sufficiently small. If it is assumed that the effect of $\mathbf{G}(\mathbf{V}_s)$ can be discounted and only one source is present then

$$\angle \mathbf{W}_{jk} = \frac{2\pi\nu}{c}(||\mathbf{v}_s - \mathbf{v}_j|| - ||\mathbf{v}_s - \mathbf{v}_k||) + 2\pi m_{jk}, \tag{8}$$

where m_{jk} is an integer that represents the phase ambiguity. Let $\boldsymbol{\delta}_i = \mathbf{v}_s^o - \mathbf{v}_j$, where $\mathbf{v}_s^o$ is an estimate of the RFI position and let the error $\boldsymbol{\varepsilon} = \mathbf{v}_s^o - \mathbf{v}_s$ (assumed small). Then the Taylor expansion yields

$$\begin{aligned} ||\mathbf{v}_s - \mathbf{v}_j|| = ||\boldsymbol{\delta}_j - \boldsymbol{\varepsilon}|| &= \sqrt{||\boldsymbol{\delta}_j||^2 + ||\boldsymbol{\varepsilon}||^2 - 2\boldsymbol{\delta}_j \cdot \boldsymbol{\varepsilon}} \\ &\approx ||\boldsymbol{\delta}_j|| - \frac{\boldsymbol{\delta}_j \cdot \boldsymbol{\varepsilon}}{||\boldsymbol{\delta}_j||}. \end{aligned} \tag{9}$$

Using the approximation in equation (9), define

$$\begin{aligned} \mathbf{B}_{jk} &= \left(\frac{-\boldsymbol{\delta}_j}{||\boldsymbol{\delta}_j||} + \frac{\boldsymbol{\delta}_k}{||\boldsymbol{\delta}_k||}\right) \cdot \boldsymbol{\varepsilon} \\ &\approx \angle\left[\mathbf{W}_{jk} e^{\frac{-i2\pi\nu}{c}(||\boldsymbol{\delta}_j|| - ||\boldsymbol{\delta}_k||)}\right] \frac{c}{2\pi\nu}, \end{aligned} \tag{10}$$

which only holds if $\boldsymbol{\varepsilon}$ is sufficiently small so that the phase ambiguity m_{jk} is zero. By stacking the transposed rows of the top triangular part of $\mathbf{B}$, an $N_b \times 1$ vector can be created

$$\mathbf{b} = \mathbf{M}\boldsymbol{\varepsilon}, \tag{11}$$

where $\mathbf{M}$ is an $N_b \times 3$ matrix consisting of the stacked $\left(\frac{-\boldsymbol{\delta}_j}{||\boldsymbol{\delta}_j||} + \frac{\boldsymbol{\delta}_k}{||\boldsymbol{\delta}_k||}\right)$ vectors. Equation (11) is then used to define the least squares (LS) problem $\widehat{\boldsymbol{\varepsilon}} = \underset{\boldsymbol{\varepsilon}}{\operatorname{argmin}} ||\mathbf{b} - \mathbf{M}\boldsymbol{\varepsilon}||^2$. The optimal solution in an LS sense is then

$$\widehat{\boldsymbol{\varepsilon}} = (\mathbf{M}^H\mathbf{M})^{-1}\mathbf{M}^H\mathbf{b}. \tag{12}$$

When equation (12) is used to calculate $\hat{\boldsymbol{\varepsilon}}$ iteratively and the estimate $\mathbf{v}_s^o := \mathbf{v}_s^o - \widehat{\boldsymbol{\varepsilon}}$ is updated, the estimate $\mathbf{v}_s^o$ will converge to $\mathbf{v}_s$ if the initial estimate for $\mathbf{v}_s$ is within the main lobe of the beamformer.

4 Simulation in the Near-field

To evaluate the proposed algorithm, a simulation was done using the layout of the 48 coplanar antennas from the LOFAR CS302 station Low Band Antenna (LBA) subsystem (see figure 1). A uniform distribution was used to generate 5000 random source positions which lie outside the aforementioned array, but within the array near-field. From the positions, covariance matrices were generated and the algorithm was applied to each one. For only 2.1 % of the covariance matrices did the integrating-out-variables method have to iterate more than once.

For 95 % of the runs, the algorithm took less than 1.5 *s* (the median of all runs was 1.16 *s* and the maximum 9 *s*). This gives a speed-up in the order of 8000 compared to the 3D MUSIC method when both methods were run on the same hardware, had the same resolution and were not parallelised.

[1] Only one hemisphere needs to be considered for an Earth based array.

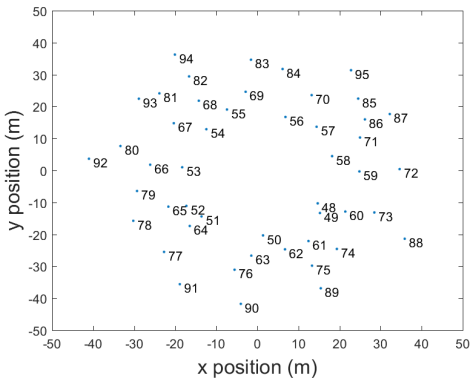

Figure 1. Array layout of the LOFAR CS302 Low Band Antenna subsystem.

To measure the accuracy of the algorithm, the euclidean distance (now called the distance error) between the position of each source and its corresponding estimated position was calculated. The integrating-out-variables stage yielded a median distance error of 2.19 *m* with a median average deviation of 1.19 *m* (see figure 2). After the convergence stage, the median as well as spread of the distance errors are drastically reduced to effectively 0. Only 1.24% of the distance errors are non-zero, however all are smaller than 3.2 *m*. These outliers all lie within 0.06 *rad* of the horizon, lie further than 170 *m* from the array centre and the error appears in the z direction (the direction orthogonal to the plane that the array lies in). This occurs because the array is planar and therefore has less resolution in the z direction for sources further away from the array and closer to the horizon (a similar loss in accuracy also occurs when using the 3D MUSIC algorithm).

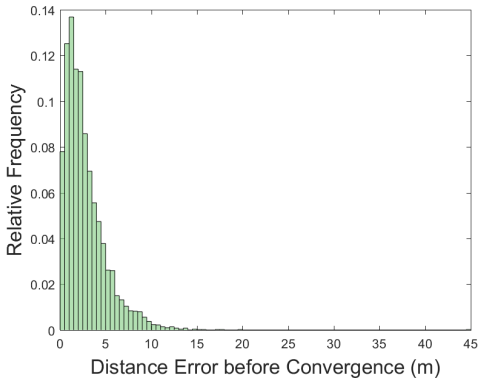

Figure 2. Relative frequency histogram of the distance error before the convergence stage for 5000 runs.

5 Conclusion

A new near-field localisation algorithm for interferometric arrays with low array beam side lobes is proposed. The algorithm is validated using simulations and has a similar accuracy to the 3D MUSIC algorithm. The advantage of the proposed algorithm is that the computational complexity is reduced from $\mathcal{O}(N_r \times N_\theta \times N_\phi)$ to $\mathcal{O}(N_r + N_\theta + N_\phi)$. The drawback is that the algorithm introduces weighting matrices that have to be calculated once a priori and stored. The algorithm has the same accuracy as 3D MUSIC. These results strongly indicate the accuracy and precision of the proposed algorithm to locate RFI sources.

6 Acknowledgements

This work is funded and supported by IBM, ASTRON, the Dutch Ministry of Economic Affairs and the Province of Drenthe, SKA-SA, the SA Research Chairs Initiative of the DST, the NRF, and a Marie Curie IRSES Fellowship within the 7th EC Framework Programme MIDPREP.

References

[1] M. P. van Haarlem et al., "LOFAR: The Low Frequency Array," *Astronomy & Astrophysics*, **556**, A2, August 2013, pp. 1–53, doi:10.1051/0004-6361/201220873.

[2] P. E. Dewdney, P. J. Hall, R. T. Schilizzi, and T. J. L. W. Lazio, "The Square Kilometre Array," *Proceedings of the IEEE*, **97**, 8, August 2009, pp. 1483-1496, doi:10.1109/JPROC.2009.2021005.

[3] D. Starer and A. Nehorai, "Passive Localization of Near-Field Sources by Path Following," *IEEE Transactions on Signal Processing*, **42**, 3, March 1994, pp. 677–680, doi:10.1109/78.277864.

[4] A. J. Weiss and B. Friedlander, "Range and Bearing Estimation Using Polynomial Rooting," *IEEE Journal of Oceanic Engineering*, **18**, 2, April 1993, pp. 130–137, doi:10.1109/48.219532.

[5] A. van der Veen, A. Leshem and A. Boonstra, "Signal Processing for Radio Astronomical Arrays," *Processing Workshop Proceedings, Sensor Array and Multichannel Signal*, July 2004, pp. 1–10, doi:10.1109/SAM.2004.1502901.

[6] M. Zatman, "How narrow is narrowband?," *IEE Proceedings-Radar, Sonar and Navigation*, **145**, 2, April 1998, pp. 85–91, doi:10.1049/ip-rsn:19981670.

[7] C. A. Balanis and P. I. Ioannides, *Introduction to Smart Antennas*, Morgan & Claypool Publishers, 2007.

[8] H. H. Hatman, *Modern Factor Analysis*, University of Chicago Press, 1976.

[9] S. J. Wijnholds, G. Pupillo, P. Bolli and G. Virone, "UAV-Aided Calibration for Commissioning of Phased Array Radio Telescopes," *URSI AP-RASC*, August 2016, pp. 228–231, doi:10.1109/URSIAP-RASC.2016.7601375.